

# Integral-equation analysis of single-site coarse-grained models for polymer-colloid mixtures

Roberto Menichetti,<sup>1,2,\*</sup> Andrea Pelissetto,<sup>1,2,†</sup> Giuseppe D'Adamo,<sup>3,‡</sup> and Carlo Pierleoni<sup>4,§</sup>

<sup>1</sup>*Dipartimento di Fisica, Sapienza Università di Roma, P.le Aldo Moro 2, I-00185 Roma, Italy.*

<sup>2</sup>*INFN, Sezione di Roma I, P.le Aldo Moro 2, I-00185 Roma, Italy.*

<sup>3</sup>*SISSA, V. Bonomea 265, I-34136 Trieste, Italy.*

<sup>4</sup>*Dipartimento di Scienze Fisiche e Chimiche, Università dell'Aquila and CNISM, UdR dell'Aquila, V. Vetoio 10, Loc. Coppito, I-67100 L'Aquila, Italy.*

We discuss the reliability of integral-equation methods based on several commonly used closure relations in determining the phase diagram of coarse-grained models of soft-matter systems characterized by mutually interacting soft and hard-core particles. Specifically, we consider a set of potentials appropriate to describe a system of hard-sphere colloids and linear homopolymers in good solvent, and investigate the behavior when the soft particles are smaller than the colloids, which is the regime of validity of the coarse-grained models. Using computer-simulation results as a benchmark, we find that the hypernetted-chain approximation provides accurate estimates of thermodynamics and structure in the colloid-gas phase in which the density of colloids is small. On the other hand, all closures considered appear to be unable to describe the behavior of the mixture in the colloid-liquid phase, as they cease to converge at polymer densities significantly smaller than those at the binodal. As a consequence, integral equations appear to be unable to predict a quantitatively correct phase diagram.

## I. INTRODUCTION

Integral-equation methods are a very powerful tool to determine the thermodynamics and the liquid structure of simple fluids [1, 2]. They rely on different approximate closure relations which, supplemented by the Ornstein-Zernike (OZ) equation, allow a direct and numerically fast determination of the pair correlation functions as well as of thermodynamic quantities like pressure, compressibility, chemical potential, . . . For simple fluids these methods cannot compete nowadays with Monte Carlo and molecular-dynamics simulations. Nonetheless, they have the advantage of providing reasonably accurate estimates of thermodynamic quantities with a very limited effort, and they are therefore a very valuable tool when the system under investigation depends on many parameters, for instance in the case of multicomponent systems. Moreover, they are still very useful for the analysis of systems for which atomistic simulations are particularly slow, for instance in glassy systems; see, e.g., Refs. [3–5].

Liquid-state integral equations have also been extensively used to compute fluid-fluid phase-coexistence lines. In the density region in which the system demixes, integral equations may not converge, or may converge to physically unacceptable solutions. The relation between the boundary of this nonconvergence region (we will call it termination line) and the binodal and the spinodal curves characterizing the two-phase unstable region has been the subject of many studies, see, e.g., Refs. [6–9]. In particular, it has been shown that, except in the case of very simple approximations, thermodynamical quantities do not show any particular divergence on this line, hence it cannot be taken as an approximate estimate of the spinodal line. However, it is usually assumed that it is somewhat close to the line where phase separation occurs.

In this paper we wish to investigate the reliability of integral-equation methods for the determination of the phase diagrams of typical coarse-grained models of soft-matter systems. We consider here a binary mixture of soft and hard spheres of different sizes with an intrinsic nonadditive nature. Although we take specific pair potentials, appropriate to describe, in a coarse-grained fashion, a binary system of hard-sphere colloids and long polymers under good-solvent conditions [10, 11], the conclusions should apply to a general class of soft-matter systems that can be modelled as mixtures of soft and/or hard

---

\*Electronic address: Roberto.Menichetti@roma1.infn.it

†Electronic address: Andrea.Pelissetto@roma1.infn.it

‡Electronic address: giuseppe.dadamo@sissa.it

§Electronic address: Carlo.Pierleoni@aquila.infn.it

spheres, interacting via short-range potentials [12–16]. The phase diagram of the coarse-grained model has been accurately determined in Ref. [17], by means of Monte Carlo simulations, for different values of the polymer-to-colloid size ratio. Here, we investigate the same problem by using integral-equation methods. We employ the hypernetted-chain (HNC), the Percus-Yevick (PY), the Rogers-Young (RY), and the reference HNC (RHNC) closures [1, 18–20]. For each of them we determine the termination line, whose position is then compared with the Monte Carlo binodal with the purpose of understanding if this line provides a reasonable approximation of the boundary of the two-phase region. For small polymer densities, we will also be able to compute by Monte Carlo simulations the bridge functions—quantities that have an intrinsic interest in liquid-state theories—which can then be compared with the approximate ones considered in the different approaches.

The paper is organized as follows. In Sec. II we define the model, report the definitions of the different closures we use, and the explicit expressions of the quantities that are considered in the paper. In Sec. III we present our results. In Sec. III A we determine the termination line for the different closures for two different values of the polymer-to-colloid size ratio  $q$ ,  $q = 0.5$  and  $q = 0.8$ . In Sec. III B we compare the integral-equation predictions for structure and thermodynamics with Monte Carlo results. In Sec. III C we determine the bridge functions with Monte Carlo methods and compare them with those used in the different integral-equation approaches. In Sec. III D we consider a novel approximation that uses the Monte-Carlo determined bridge functions. Finally, in Sec. IV we draw our conclusions. Technical details are reported in Appendix A. The explicit expressions of the potentials are reported in Appendix B.

## II. DEFINITIONS

### A. The model

We consider a mixture of mutually interacting hard spheres of radius  $R_c$  and of soft particles with a typical interaction range  $R_g$ . Specifically, we consider here a set of potentials which are appropriate to describe a system of hard-sphere colloids of size  $R_c$  and linear homopolymers in good solvent of radius of gyration  $R_g$ , after tracing out the monomer degrees of freedom and replacing each chain with a particle coinciding with its center of mass. The coarse-grained model is accurate only if polymers are dilute, i.e., for  $\Phi_p = 4\pi N_p R_g^3 / (3V) \lesssim 1$  ( $N_p$  is the number of colloids in the volume  $V$ ), and if the polymer-to-colloid size ratio  $q = R_g/R_c$  satisfies  $q \lesssim 1$  [17, 28] (a discussion of the accuracy of the model, with a comparison with full-monomer results is presented in Ref. [17]).

Polymer-colloid solutions have been extensively studied [21–26], because of their rich phase diagram, which presents fluid-fluid and fluid-solid coexistence lines, and because of their technological relevance [27]. In this paper, we will not be interested in using the model to predict their phase behavior. Rather, we take it as a typical soft-matter system and use it as reference model for which we can study the predictivity of the different closures that are typically used in integral-equation studies. We will consider three different values of  $q = R_g/R_c$ ,  $q = 0.5, 0.8$ , and  $1$ . The corresponding pair potentials have been determined in several papers [29–34]. Here we shall use the accurate scaling-limit results of Refs. [32, 34].

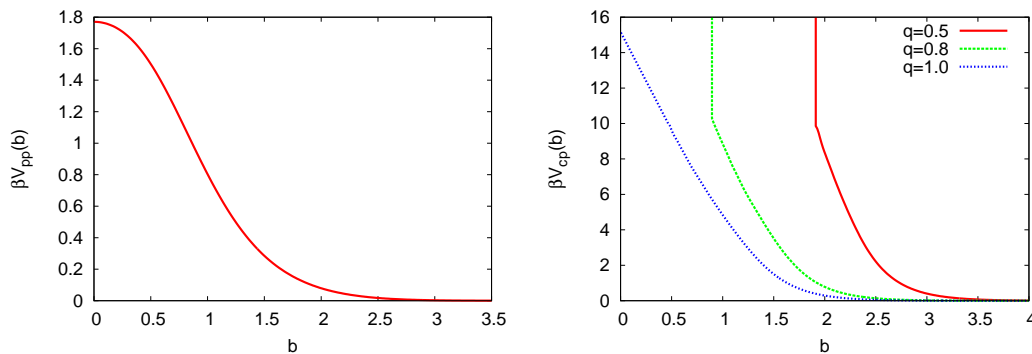


FIG. 1: Left: polymer-polymer pair potential  $\beta V_{pp}(b)$  as a function of  $b = r/R_g$ ; right: polymer-colloid potential  $\beta V_{cp}(b; q)$  as a function of  $b = r/R_g$  for  $q = 0.5, 0.8, 1$ . For  $q = 0.8$  and  $q = 0.5$ , we assume  $V_{cp}(b; q) = \infty$  for  $b < 0.90, 1.91$ , respectively.

They are reported for completeness in Appendix B and shown in Fig. 1. The polymer-polymer potential is essentially Gaussian with  $V_{pp}(b=0) \approx 1.8k_B T$  at full overlap. On the other hand, the nature of the polymer-colloid potential depends on  $q$ . For  $q \leq 1$  the potential is expected to be infinite at full overlap and very large for  $r \lesssim R_c = R_g/q$ . Then, it decays fast, with a tail that is small for  $r \gtrsim R_c + 2R_g$ . Note that we have not been able to determine  $\beta V_{cp}(b; q)$  in the small- $r$  region in which  $\beta V_{cp}(b; q) \gtrsim 10$ . For these values of  $r$  we simply assume  $\beta V_{cp}(b; q) = +\infty$  for  $q = 0.5$  and  $q = 0.8$ . For  $q = 1$  we performed a linear extrapolation.

## B. Closure relations

In the integral-equation approach the basic ingredients are the pair correlation functions  $h_{\alpha\beta}(r)$  ( $\alpha$  and  $\beta$  label the two species) and the direct correlation functions  $c_{\alpha\beta}(r)$ . They are related by the Ornstein-Zernike (OZ) [1] relations

$$\hat{h}_{\alpha\beta}(k) = \hat{c}_{\alpha\beta}(k) + \sum_{\gamma} \hat{c}_{\alpha\gamma}(k) \rho_{\gamma} \hat{h}_{\gamma\beta}(k), \quad (1)$$

where we denote with  $\hat{f}(k)$  the (three-dimensional) Fourier transform of any function  $f(r)$ . To compute the quantities of interest, the OZ relation must be supplemented by a closure relation, which can be written in general form as

$$g_{\alpha\beta}(r) = e^{-\beta V_{\alpha\beta}(r)} \exp[h_{\alpha\beta}(r) - c_{\alpha\beta}(r) + b_{\alpha\beta}(r)], \quad (2)$$

where  $V_{\alpha\beta}(r)$  are the pair potentials,  $g_{\alpha\beta}(r) = h_{\alpha\beta}(r) + 1$  is the pair distribution function and  $b_{\alpha\beta}(r)$  is the so-called bridge function. The latter quantity cannot be computed exactly, hence we consider several different approximations:

(i) Hypernetted chain (HNC) closure [1]. We simply set  $b_{\alpha\beta}(r) = 0$  for all  $\alpha, \beta$ . This approximation is very accurate for soft potentials [1].

(ii) Mixed HNC/Percus-Yevick (PY) closure. For hard spheres the PY closure relation [1]

$$g_{\alpha\beta}(r) = e^{-\beta V_{\alpha\beta}(r)} [1 + h_{\alpha\beta}(r) - c_{\alpha\beta}(r)] \quad (3)$$

is more accurate than the HNC closure. Here we consider the HNC closure for polymer-polymer and polymer-colloid correlations and the PY closure for the colloid-colloid correlations.

(iii) Rogers-Young (RY) closure [18, 35]. This closure mixes the HNC and the PY closures, adding free parameters that are tuned to obtain thermodynamic consistency. It is defined by

$$g_{\alpha\beta}(r) = e^{-\beta V_{\alpha\beta}(r)} \left[ 1 + \frac{\exp[(h_{\alpha\beta}(r) - c_{\alpha\beta}(r))f_{\alpha\beta}(r)] - 1}{f_{\alpha\beta}(r)} \right], \quad (4)$$

where the function  $f_{\alpha\beta}(r)$  is given by

$$f_{\alpha\beta} = 1 - e^{-\chi_{\alpha\beta} r}. \quad (5)$$

Note that, for  $\chi_{\alpha\beta} \rightarrow 0$  we recover the PY closure, while in the opposite limit,  $\chi_{\alpha\beta} \rightarrow \infty$ , we reobtain the HNC closure. In most of the discussion we have considered a single optimization parameter, setting  $\chi_{\alpha\beta} = \chi/s_{\alpha\beta}$ ,  $s_{cc} = R_c$ ,  $s_{pp} = R_g$ ,  $s_{pc} = (R_c + R_g)/2$ . The parameter  $\chi$  has been determined as discussed below.

(iv) Reference HNC (RHNC) closure [19, 20]. In this approach one sets  $b_{\alpha\beta}(r) = b_{\alpha\beta}^{HS}(r; R_p, R_c)$ , where the latter quantities are the bridge functions of a system of additive hard spheres of radii  $R_p$  and  $R_c$  at the same densities of the polymers and colloids in the original system. The polymer effective radius  $R_p$  is determined by using the Lado criterion [20, 36]

$$\sum_{\alpha\beta} x_{\alpha} x_{\beta} \int_0^{\infty} r^2 dr [h_{\alpha\beta}(r) - h_{\alpha\beta}^{HS}(r; R_p, R_c)] \frac{\partial b_{\alpha\beta}^{HS}(r; R_p, R_c)}{\partial R_p} = 0, \quad (6)$$

where  $x_{\alpha} = N_{\alpha}/(N_c + N_p) = \rho_{\alpha}/(\rho_p + \rho_c)$ . The bridge functions  $b_{\alpha\beta}^{HS}(r; R_p, R_c)$  can be computed as discussed in Refs. [20, 37–43].

Solving simultaneously the OZ and the closure relations, one obtains  $h_{\alpha\beta}(r)$  and  $c_{\alpha\beta}(r)$ . Then, one can use them to compute thermodynamic quantities.

### C. Observables

We will be interested in computing the pressure. One possibility consists in using the virial expression:

$$\beta P^{(\text{vir})} = \rho \left( 1 + \sum_{\alpha\beta} Z_{\alpha\beta} \right), \quad (7)$$

where  $\beta = 1/k_B T$ ,  $\rho = \rho_p + \rho_c$ , and the quantities  $Z_{\alpha\beta}$  are given by

$$Z_{\alpha\beta} = -\frac{2\pi}{3\rho} \rho_\alpha \rho_\beta \int_0^\infty r^3 dr \frac{\partial \beta V_{\alpha\beta}}{\partial r} g_{\alpha\beta}(r). \quad (8)$$

This expression cannot be applied to hard spheres, since the potential is discontinuous. In this case we have

$$Z_{cc} = \frac{16\pi R_c^3}{3\rho} \rho_c^2 g_{cc}(2R_c). \quad (9)$$

Eq. (8) is also not convenient in the polymer-colloid case as  $\beta V_{pc}(r)$  diverges as  $r \rightarrow 0$ . In the HNC case, this problem can be overcome by rewriting Eq. (8) as

$$Z_{\alpha\beta} = \frac{2\pi}{3\rho} \rho_\alpha \rho_\beta \int_0^\infty r^3 dr \frac{\partial e^{-\beta V_{\alpha\beta}}}{\partial r} e^{h_{\alpha\beta}(r) - c_{\alpha\beta}(r)}. \quad (10)$$

A similar formula can be analogously obtained in the case of the RY closure.

Another quantity we shall be interested in is the isothermal compressibility  $\kappa_T$  that can be either computed by using the virial route

$$\frac{\beta}{\kappa_T} = \left( \frac{\partial \beta P^{(\text{vir})}}{\partial \rho_p} \right)_{\rho_c} \rho_p + \left( \frac{\partial \beta P^{(\text{vir})}}{\partial \rho_c} \right)_{\rho_p} \rho_c \quad (11)$$

or as [44]

$$\frac{\beta}{\kappa_T} = \rho - \sum_{\alpha\beta} \rho_\alpha \rho_\beta \hat{c}_{\alpha\beta}(0). \quad (12)$$

The two expressions are thermodynamically equivalent. However, when an approximate closure is used, two different results are obtained, as a consequence of the thermodynamic inconsistency of the approach. In the RY case, the parameter  $\chi$  is fixed so that the two different routes provide the same result for  $\kappa_T$ .

Finally, we shall consider the structure factors

$$S_{\alpha\beta}(k) = \delta_{\alpha\beta} + \sqrt{\rho_\alpha \rho_\beta} \hat{h}_{\alpha\beta}(k), \quad (13)$$

and the concentration structure factor

$$S_c(k) = x_p x_c [x_p S_{cc}(k) + x_c S_{pp}(k) - 2\sqrt{x_p x_c} S_{cp}(k)]. \quad (14)$$

For  $k \rightarrow 0$ ,  $1/S_c(k) \rightarrow \partial^2 \beta g(x_p, P) / \partial x_p^2$ , where  $g(x_p, P)$  is the Gibbs free energy per particle. Hence, its divergence signals the thermodynamic instability of the homogeneous phase.

## III. RESULTS

In order to solve the coupled integral equations, the correlation functions are discretized on a regular grid. We usually take a step size  $\Delta r/R_g = 10^{-3}$  and truncate the correlation functions at  $R_{\text{max}}/R_g = N\Delta r$ , with  $N = 32768$ . As we discuss in appendix A, these choices make truncation and discretization errors negligible. We use the standard Picard iterative method, which converges quite fast, except close to the termination line. We improve convergence by considering a mixing parameter  $\alpha$ . If  $c_{\text{ini}}^{(n)}(r)$  and  $c_{\text{end}}^{(n)}(r)$  indicate the direct correlation functions at the beginning and at the end of the  $n$ -th step of the iterative procedure, respectively, we set  $c_{\text{ini}}^{(n+1)}(r) = (1 - \alpha)c_{\text{ini}}^{(n)}(r) + \alpha c_{\text{end}}^{(n)}(r)$ . Far from the termination line,  $\alpha$  is not a relevant parameter. However, close to the termination line, convergence is only obtained if  $\alpha$  is small. In some cases, we took  $\alpha \sim 10^{-2}$ .

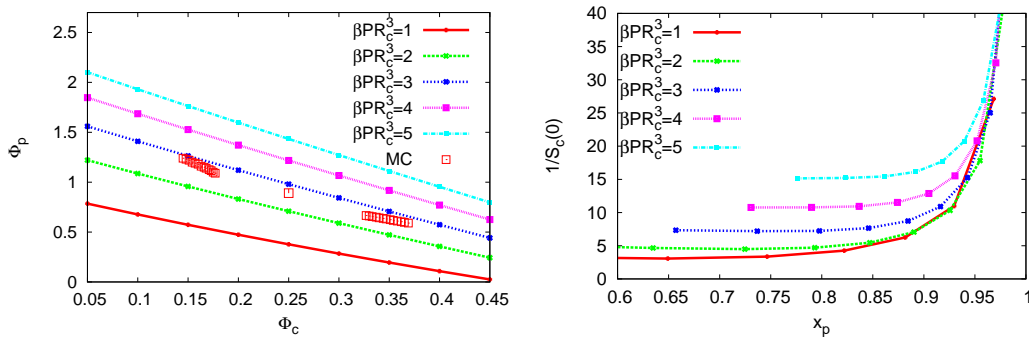


FIG. 2: Results for  $q = 0.8$  and the HNC/PY closure (in this case there is no termination line). Left: isobars corresponding to  $\beta PR_c^3 = 1, 2, 3, 4,$  and  $5$  in the  $\Phi_c, \Phi_p$  plane. We also report the Monte Carlo estimates of the binodal (empty squares, MC). Note that isobars with  $\beta PR_c^3 \geq 3$  go through the two-phase region. Right:  $1/S_c(k=0)$  along the same isobars reported in the left panel as a function of  $x_p = N_p/(N_p + N_c)$ .

### A. Termination lines

In order to determine the termination line, we work as follows. We fix the colloid volume fraction  $\Phi_c$  ( $\Phi_c = 4\pi R_c^3 N_c/3V$ , where  $N_c$  is the number of colloids present in the box of volume  $V$ ) and solve the equations for a small value of the polymer density. Typically, if  $\Phi_p = 4\pi R_g^3 N_p/3V$  ( $N_p$  is the number of polymers present in the box of volume  $V$ ), we start at  $\Phi_p \approx 0.005$  for  $\Phi_c \gtrsim 0.2$  and at  $\Phi_p \approx 0.01$  for smaller colloid volume fractions. Then, we increase  $\Phi_p$  by steps  $\Delta\Phi_p$ .

For  $q = 1$  we have been able to increase  $\Phi_p$  up to 2.5 for all values of  $\Phi_c \leq 0.45$ : We always find a regular solution of the integral equations. This is not surprising, as, for this value of  $q$ , Monte Carlo simulations indicate that the fluid-fluid binodal either does not exist or is located at quite large values of the polymer volume fraction. In particular, Ref. [17] found no phase transition up to  $\Phi_p = 2.12, 1.73, 1.33$  for  $\Phi_c = 0.1, 0.2, 0.3$ , respectively.

For  $q = 0.8$  integral equations do not show any singular behavior if the HNC/PY closure is used. Also in this case we have been able to solve the equations for any  $\Phi_p \leq 2.5$  and  $\Phi_c \leq 0.45$ . No phase demixing is observed, as it is evident from the behavior of  $1/S_c(k=0)$  along five different isobars shown in Fig. 2. At the critical point  $1/S_c(k=0)$  should vanish. Instead, it increases as the pressure  $P$  is increased, with no indication of a zero for some values of  $P$  and  $x_p$ . Apparently, the HNC/PY closure fails even in reproducing the qualitative behavior of the system.

TABLE I: For each  $q$  and  $\Phi_c$  (first two columns), we report the polymer volume fraction  $\Phi_p$  at which integral equations no longer converge to a physical solution for three different closures: HNC, HNC/PY, and RY. In the last column we report the polymer volume fraction  $\Phi_p^{\text{bin}}$  at which the binodal, as computed by Monte Carlo simulations [17], occurs. We have also computed the termination line for the RHNC closure, for  $q = 0.5$  and  $\Phi_c = 0.3$ :  $\Phi_p = 0.104$ .

$q$	$\Phi_c$	HNC	HNC/PY	RY	$\Phi_p^{\text{bin}}$
0.5	0.10	0.87	$\geq 2.5$	0.88	0.69
	0.20	0.23	$\geq 2.5$	0.34	0.53
	0.30	0.090	0.15	0.18	0.38
	0.40	0.036	0.07	0.115	0.255
0.8	0.10	$\geq 2.5$	$\geq 2.5$	$\geq 2$	
	0.20	0.61	$\geq 2.5$	$\geq 2$	1.0
	0.30	0.175	$\geq 2.5$	0.39	0.75
	0.40	0.086	$\geq 2.5$	0.29	$0.5 \leq \Phi_p \leq 0.6$

For  $q = 0.8$  a termination line is observed if we use the HNC or the RY closures, while for  $q = 0.5$  a no-convergence domain is observed also by using the HNC/PY closure. Results for the termination

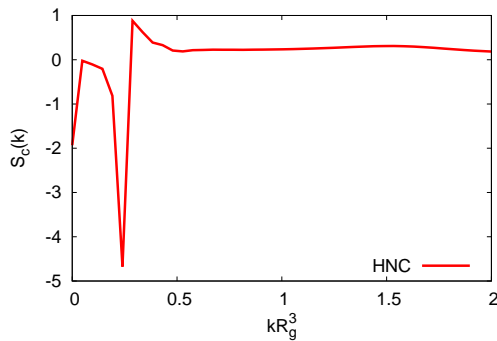


FIG. 3: Estimate of  $S_c(k)$  for  $\Phi_c = 0.3$  and  $\Phi_p = 0.0905$ , on the termination line. Here  $q = 0.5$  and we use the HNC closure.

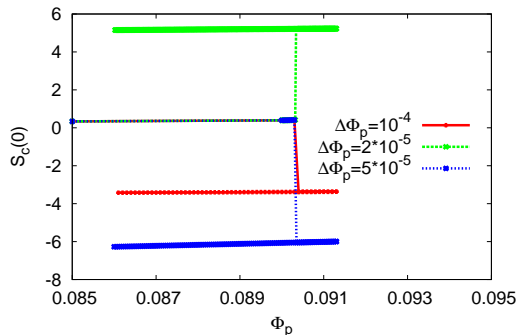


FIG. 4: Estimate of  $S_c(k=0)$  for three different  $\Delta\Phi_p$  and the HNC closure. We start from the values of  $c_{\alpha\beta}(r)$  and  $h_{\alpha\beta}(r)$  for  $\Phi_p = 0.9$  and increase  $\Phi_p$  by steps  $\Delta\Phi_p$  up to  $\Phi_p = 0.0915$ , then we decrease  $\Phi_p$  with the same schedule up to  $\Phi_p = 0.086$ . The termination line occurs for  $\Phi_p = 0.0903$ .

lines for both values of  $q$  are reported in Table I. The termination line is determined as follows. Starting from the initial value  $\Phi_p^{(0)}$ , we subsequently solve the equations for  $\Phi_p^{(n)} = \Phi_p^{(0)} + n\Delta\Phi_p$ , starting the iterations for the  $n$ -th density from the solution at  $\Phi_p^{(n-1)}$ . If  $\Delta\Phi_p$  is large or the mixing parameter in the Picard iterations is of order 1, we end up at a density  $\Phi_p^{(M)}$  where the iterations no longer converge. Then, we consider again the solution at  $\Phi_p^{(M-1)}$ , but now we significantly decrease  $\Delta\Phi_p$  and the mixing parameter (typically we take a parameter as small as 0.01). If we increase again  $\Phi_p$ , we now observe that the Picard iterations always converge. However, at a very specific value of  $\Phi_p$  the stable solution is no longer physical, as  $S_c(k)$  becomes discontinuous at a finite value of  $k$ . We identify the termination line as the smallest polymer density at which  $S_c(k)$  (the same occurs for all structure factors  $S_{\alpha\beta}(k)$ ) develops a discontinuity. An example is shown in Fig. 3, where we report  $S_c(k)$  for  $q = 0.5$ ,  $\Phi_c = 0.3$ ,  $\Phi_p = 0.0903$ , as obtained by using the HNC closure. It is interesting to observe that while the position of the termination line is independent of the protocol used to increment  $\Phi_p$ , the singular solution depends on  $\Delta\Phi_p$ . For instance, in Fig. 4 we show the estimates of  $S_c(k=0)$  as a function of  $\Phi_p$  for three different values of  $\Delta\Phi_p$ . Incrementing  $\Phi_p$ , at the termination line  $\Phi_p = 0.0903$  we always observe a jump in  $S_c(0)$  to a new value. However, such value depends on  $\Delta\Phi_p$ . If we further increase  $\Phi_p$  beyond the termination line and then decrease again  $\Phi_p$ , the unphysical solution appears to be stable: The structure factor changes smoothly with  $\Phi_p$ . Moreover, once  $\Phi_p$  is again below the termination-line value, if we use a small mixing parameter, we always obtain the unphysical solution.

The termination lines for the different closures are reported in Fig. 5. In general, we find that the RY closure performs better than the HNC one, which stops converging at very small values of  $\Phi_p$  in the colloid-liquid phase. In all cases, however, the termination line is significantly below the correct binodal, especially in the colloid-liquid phase  $\Phi_c \gtrsim 0.25$ . Clearly, the convergence to an unphysical solution is not

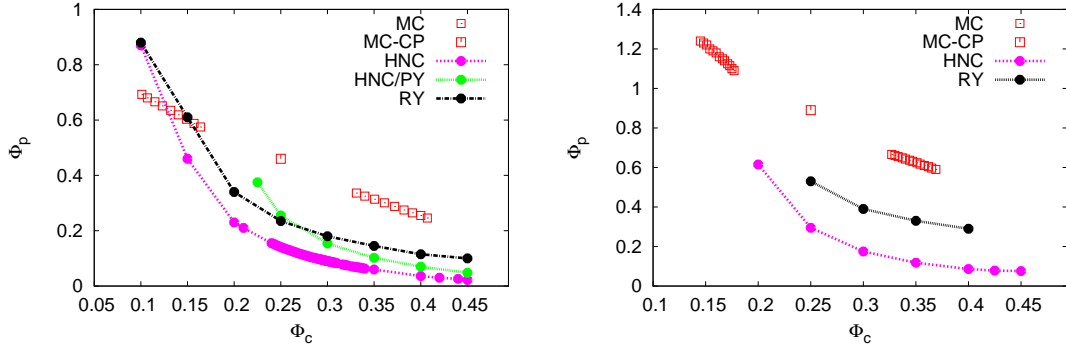


FIG. 5: Phase diagram for  $q = 0.5$  (left) and  $q = 0.8$  (right). We report the binodals obtained by Monte Carlo simulations (MC), the corresponding critical point (MC-CP), and the termination lines for each of the closures.

directly related to singularities in the thermodynamic behavior of the model. Therefore, the termination line provides a very poor approximation of the phase-separation line.

Let us finally consider the RHNC closure. Since this approach is quite complex, we have only analyzed one case:  $q = 0.5$  and  $\Phi_c = 0.3$ . For  $\Phi_p \approx 0$ , the effective radius  $R_p$  is equal to  $0.837R_g$ . This is a completely reasonable value, indicating that polymers are effectively equivalent to hard spheres of radius approximately equal to  $R_g$ . As  $\Phi_p$  increases, the effective radius  $R_p$  decreases quite rapidly: for  $\Phi_p = 0.1$  we find  $R_p = 0.60R_g$ . Again, this is consistent with intuition, as we expect the polymer to shrink as  $\Phi_p$  increases. Unfortunately, we are not able to go much beyond  $\Phi_p = 0.1$ , as the RHNC equations cease to converge at  $\Phi_p = 0.104$ . Hence, this approach represents only a modest improvement with respect to the HNC approach (the HNC termination line occurs at  $\Phi_p = 0.090$ ).

## B. Structural behavior in the homogeneous phase

We wish now to compare the integral-equation predictions with the Monte Carlo ones in the homogeneous phase. We consider the case  $q = 0.5$ , in which a termination line occurs for all considered closure relations. We begin by analyzing the structure factors  $S_{\alpha\beta}(k=0)$ , which are directly related to thermodynamics by the compressibility equations [1, 44]. In Fig. 6 we report the corresponding estimates for two values of  $\Phi_c$ ,  $\Phi_c = 0.1$  and  $0.3$ , that lie on opposite sides with respect to the critical point located at  $\Phi_{c,\text{crit}} = 0.25$ ,  $\Phi_{p,\text{crit}} = 0.46$ , as estimated by Monte Carlo simulations [17].

For  $\Phi_c = 0.1$  the HNC/PY closure significantly underestimates the structure factors. Clearly,  $|S_{\alpha\beta}(0)|$  increases too slowly as  $\Phi_p$  increases, explaining why convergence is observed at least up to  $\Phi_p = 2.5$ , see Table I. The HNC and RY estimates increase faster. The latter are more accurate than the HNC ones for small densities, but they significantly underestimate  $|S_{\alpha\beta}(0)|$  close to the binodal, which is located at  $\Phi_p \approx 0.70$  [17]. The fact that the RY results are less accurate than the HNC ones near the binodal may be surprising, as the RY closure is a generalization of the HNC closure. It simply indicates that the requirement of thermodynamic consistency does not necessarily lead to more accurate results. Note that both HNC and RY integral equations also converge for some values of  $\Phi_p$  in the metastable region beyond the binodal, see Fig. 5. In this domain the structure factors  $S_{\alpha\beta}(0)$  are quite large [on the binodal, Monte Carlo simulations give  $S_{pp}(0) = 11.5(6)$ ,  $S_{cp}(0) = -6.7(4)$ ,  $S_{cc}(0) = 4.2(2)$ ]. Therefore, even though we do not observe an exact divergence of  $S_{\alpha\beta}(k=0)$ , for this value of  $\Phi_c$  we can take the termination line as a good estimate of the spinodal.

For  $\Phi_c = 0.3$  the behavior is quite different and the termination lines occur at values of  $\Phi_p$  significantly smaller than that of the binodal. Moreover, integral equations stop converging when the structure factors  $|S_{\alpha\beta}(0)|$  are relatively small, at least if compared with the values they assume on the binodal at  $\Phi_c = 0.1$ . For instance, the HNC and HNC/PY equations both cease to converge when  $S_{pp}(0) \approx 3$ , while  $S_{pp}(0) \approx 5$  on the RY termination line. Comparing the integral-equation estimates with the Monte Carlo results, we see that the RY closure is here the most accurate, in agreement with previous studies [13, 16], although it fails to converge well before the binodal. As for the RHNC, the estimates of  $S_{cc}(0)$  and  $S_{cp}(0)$  are consistent with the RY ones and the Monte Carlo data up to  $\Phi_p \approx 0.08$ . On the other hand, the RHNC

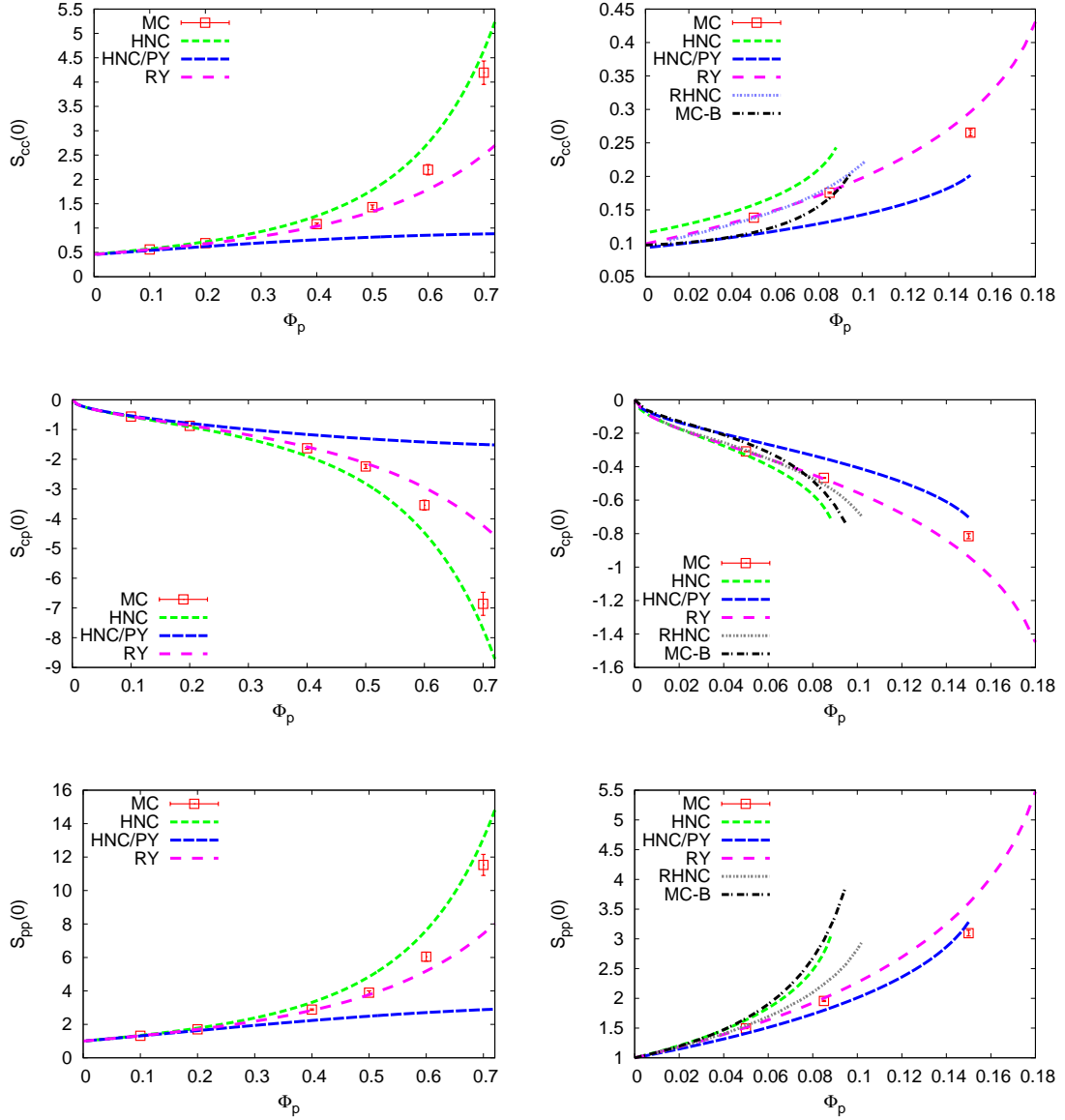


FIG. 6: Structure factors  $S_{\alpha\beta}(k=0)$  for  $q = 0.5$  and  $\Phi_c = 0.1$  (left) and  $\Phi_c = 0.3$  (right). Lines are the results obtained by using the HNC, HNC/PY, and RY closures. Symbols are Monte Carlo data. For  $\Phi_c = 0.3$  we also include results for the RHNC closure and results obtained by using the zero-polymer-density Monte Carlo bridge functions (MC-B), as discussed in Sec. III D.

estimates of  $S_{pp}(0)$  increase too fast for  $\Phi_p \gtrsim 0.04$ , looking similar to the HNC estimates. Also in this case the termination line occurs for  $S_{pp}(0) \approx 3$ .

As a second test let us compare the pair distribution functions. For  $\Phi_c = 0.1$  and  $\Phi_p = 0.7$ , i.e. on the binodal, see Fig. 7, all closures reasonably reproduce the polymer-polymer distribution function. Deviations are instead observed for the polymer-colloid and especially for the colloid-colloid distribution function. The largest deviations are observed for the HNC/PY closure. For instance, the colloid-colloid correlation is significantly underestimated at contact. While an extrapolation of the Monte Carlo data predicts  $g_{cc}(2R_c) \approx 13-14$ , we estimate  $g_{cc}(2R_c) \approx 4$  by using the HNC/PY closure. The RY closure performs better, although it is also unable to predict the correct value of  $g_{cc}(r)$  at contact and slightly overestimates  $g_{cp}(r)$  at the first peak. As for the structure factors, the HNC closure is the most accurate one for this value of  $\Phi_c$ , as the HNC curves fall on top of the Monte Carlo data.

At  $\Phi_c = 0.3$  the behavior is quite different, see Fig. 7. For  $\Phi_p = 0.085$ , close to the HNC termination



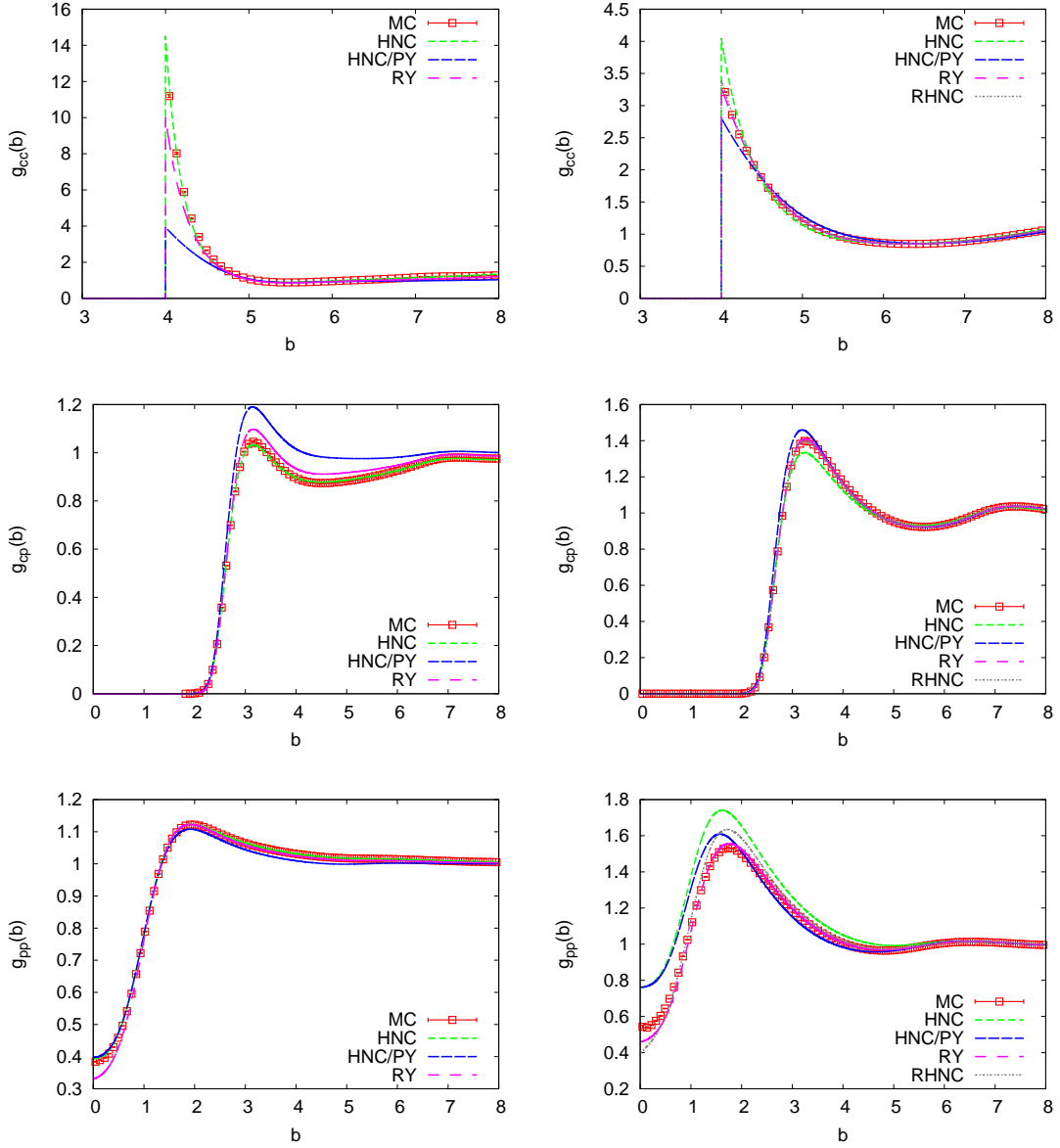


FIG. 7: Pair correlation functions  $g_{\alpha\beta}(r)$  as a function of  $b = r/R_g$  for  $q = 0.5$  at two different state points:  $\Phi_c = 0.1$ ,  $\Phi_p = 0.70$  (left) and  $\Phi_c = 0.3$ ,  $\Phi_p = 0.085$  (right). Lines are the results obtained by using the HNC, HNC/PY, RY, RHNC closures. Symbols are Monte Carlo data.

line, HNC results are not accurate, especially for  $g_{pp}(r)$ , which is significantly overestimated for  $r \lesssim 2R_g$ . The value of  $g_{cc}(r)$  at contact is also significantly overestimated. The HNC/PY closure gives results that are only marginally better than the HNC ones, while the RY estimates are in full agreement with the Monte Carlo data. The RHNC estimates of  $g_{cc}(r)$  and  $g_{cp}(r)$  are in agreement with the data, but this is not the case for  $g_{pp}(r)$ , which is overestimated for  $1 \lesssim r/R_g \lesssim 2$ , the region in which the correlation function shows the first peak. At  $\Phi_p = 0.15$  we only have RY data, as integral equations no longer converge for the other closures. The results are reported in Fig. 8. Pair correlations  $g_{cc}(r)$  and  $g_{cp}(r)$  are well reproduced, while relatively small deviations are observed for  $g_{pp}(r)$ . Apparently, RY estimates are relatively accurate even close to the corresponding termination line, located at  $\Phi_p = 0.18$ .

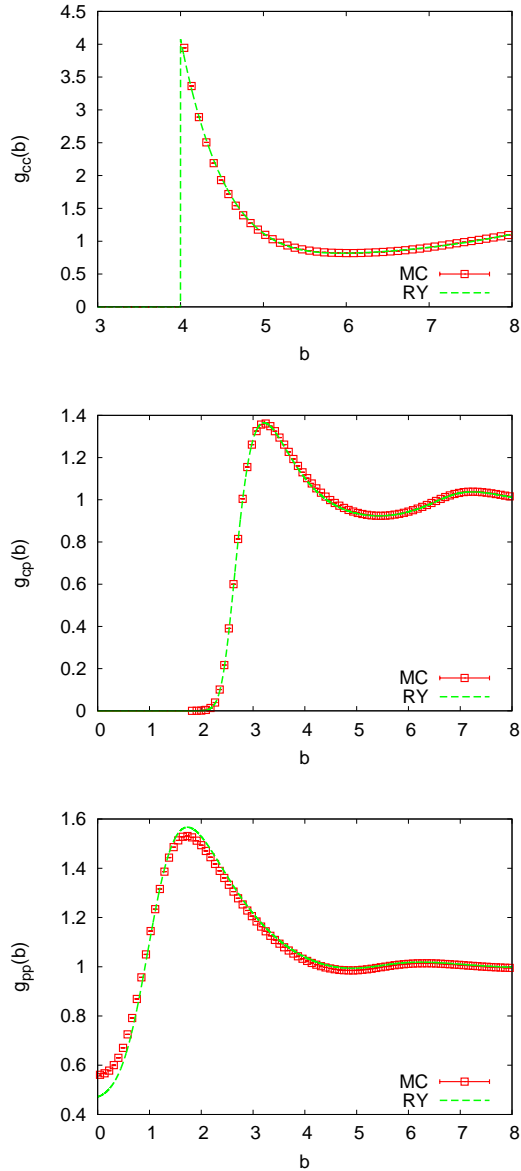


FIG. 8: Pair correlation functions  $g_{\alpha\beta}(r)$  as a function of  $b = r/R_g$  for  $q = 0.5$  at  $\Phi_c = 0.3$ ,  $\Phi_p = 0.15$ . Lines are the results obtained by using the RY closure. Symbols are Monte Carlo data.

### C. Bridge functions at zero polymer density

The failure of integral-equation methods to reproduce the thermodynamics for  $\Phi_c \gtrsim 0.2$  and to provide a reasonably accurate estimate of the boundary of the two-phase region clearly indicates that none of the closures we used is appropriate for the problem at hand. To understand better the origin of the discrepancies, we now compare the bridge functions used in the integral-equation approach with the exact estimates obtained numerically, by using the MC results for the pair correlation functions. For this purpose we should compute  $g_{\alpha\beta}(r)$  accurately on large boxes. It turns out that this is feasible only for  $\Phi_p \rightarrow 0$ , the case we will study below.

The input numerical quantities are  $g_{cc}(r)$  (we use the accurate expressions that can be obtained as discussed in Refs. [20, 39]),  $g_{cp}(r)$ , and  $g_{pp}(r)$ . To determine the last two quantities, we perform simulations for different values of  $\Phi_p$  on systems of linear size  $L/R_g = 32, 24$  for  $q = 0.5$  and 1, and perform an extrapolation to  $\Phi_p \rightarrow 0$ . Then, we determine the direct correlation functions by inverting the OZ

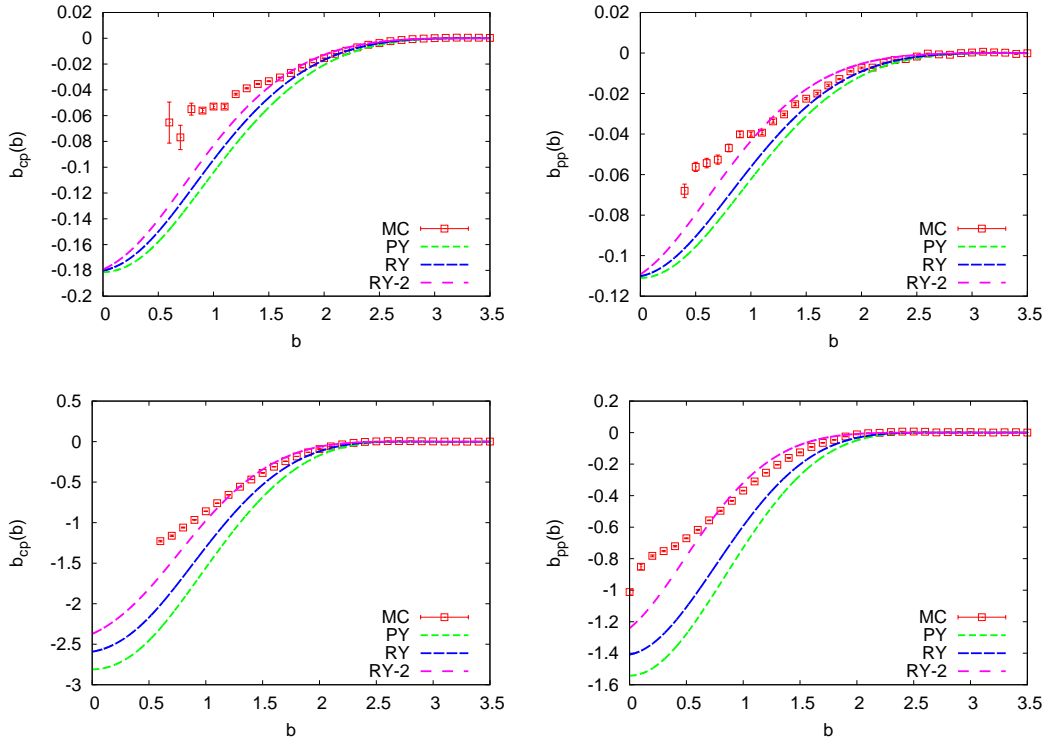


FIG. 9: Bridge functions for  $q = 1$  as a function of  $b = r/R_g$ : on the left we report  $b_{cp}(r)$ , on the right  $b_{pp}(r)$ . Top:  $\Phi_c = 0.1$ ; bottom:  $\Phi_c = 0.3$ . We report the Monte Carlo estimates (MC) as well as those obtained by using the different closures. RY-2 labels the results obtained by using the two-parameter RY closure discussed in the text.

relations, which, for  $\Phi_p \rightarrow 0$ , simplify to

$$\begin{aligned}
 \hat{c}_{cc}(k) &= \frac{\hat{h}_{cc}(k)}{1 + \rho_c \hat{h}_{cc}(k)}, \\
 \hat{c}_{cp}(k) &= \hat{h}_{cp}(k) - \rho_c \hat{c}_{cc}(k) \hat{h}_{cp}(k), \\
 \hat{c}_{pp}(k) &= \hat{h}_{pp}(k) - \rho_c \hat{c}_{cp}(k) \hat{h}_{cp}(k).
 \end{aligned} \tag{15}$$

Finally, we define

$$b_{\alpha\beta}(r) = \ln \left[ g_{\alpha\beta}(r) e^{\beta V_{\alpha\beta}(r)} \right] + c_{\alpha\beta}(r) - h_{\alpha\beta}(r). \tag{16}$$

We will focus on the polymer-polymer and colloid-polymer functions, as  $b_{cc}(r)$  depends only on the hard-sphere fluid, a case that has already been extensively discussed in the literature. Note that  $\beta V_{cp}(r)$  is large for  $r \lesssim R_c$ , so that  $g_{\alpha\beta}(r)$  is not determined accurately for these distances. Hence, we are not able to obtain reliable estimates of  $b_{cp}(r)$  for  $r \lesssim R_c$ .

For the HNC or the HNC/PY closure, we have  $b_{cp}(r) = b_{pp}(r) = 0$ . In all other cases, the bridge functions are obtained from Eq. (16), using the correlation functions obtained by means of the different closures. For the values of  $r$  for which  $V_{cp}(r)$  is large, it is convenient to express  $g_{cp}(r) e^{\beta V_{cp}(r)}$  in terms of  $h_{cp}(r) - c_{cp}(r)$  using the closure relation. This trick allows us to compute the bridge functions  $b_{cp}(r)$  inside the core region  $r \lesssim R_c$ , although here they cannot be compared with the Monte Carlo results. In this section we do not consider the HNC/PY, as it has the same bridge functions of the HNC closure. We will instead discuss the full PY closure, in which Eq. (3) is used for all correlations.

The bridge functions for  $\Phi_c = 0.1$  and  $0.3$  are reported in Figs. 9 and 10 for  $q = 1$  and  $0.5$ , respectively. For  $\Phi_c = 0.1$  the bridge functions are tiny, explaining why the HNC closure works reasonably well. The PY and RY closures are essentially equivalent. Small deviations are evident for  $q = 1$  and  $r \lesssim 2R_g$  — but in this range data become increasingly less accurate — while for  $q = 0.5$  no deviations are observed in

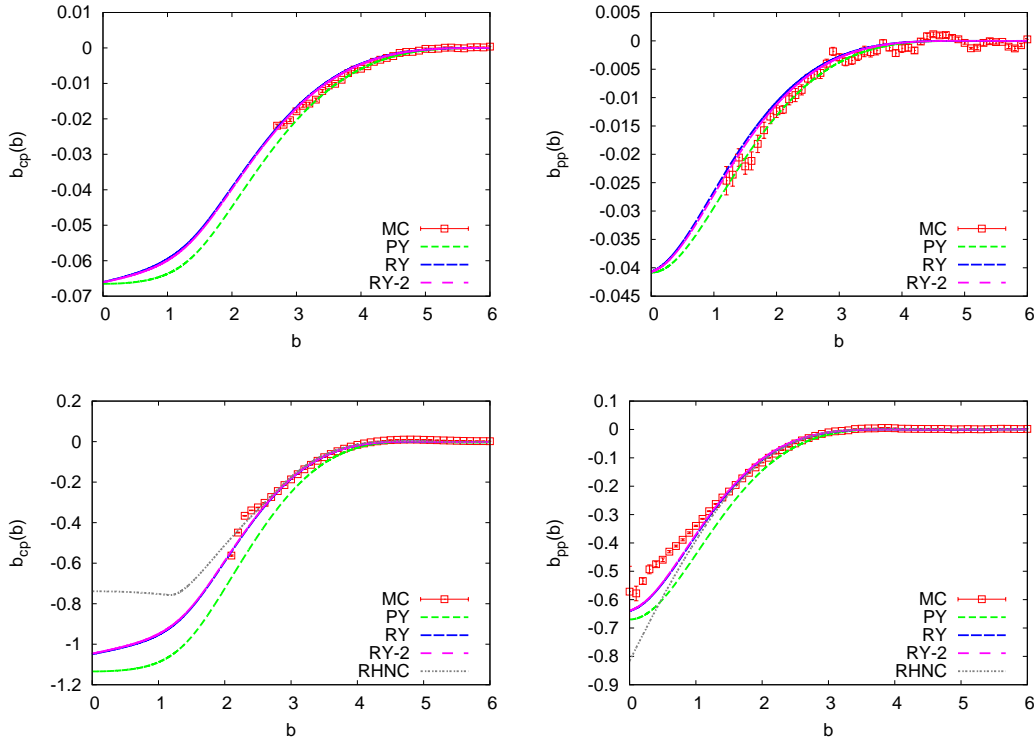


FIG. 10: Bridge function for  $q = 0.5$  as a function of  $b = r/R_g$ : on the left we report  $b_{cp}(r)$ , on the right  $b_{pp}(r)$ . Top:  $\Phi_c = 0.1$ ; bottom:  $\Phi_c = 0.3$ . We report the Monte Carlo estimates (MC) as well as those obtained by using the different closures. RY-2 labels the results obtained by using the two-parameter RY closure discussed in the text.

the region in which data appear to be reliable. As  $\Phi_c$  increases, the bridge functions become increasingly negative for small values of  $r$ . For  $q = 1$  and  $\Phi_c = 0.3$ , none of the closures appear to be accurate, although the RY closure is marginally better, and large deviations are observed for  $r \lesssim 2R_g$ . For  $q = 0.5$  the RY closure reproduces well  $b_{cp}(r)$  up to  $r \approx 2R_g$ —the region outside the colloid core. On the other hand, deviations are clearly observed for  $b_{pp}(r)$  when  $r \lesssim R_g$ . The PY closure is clearly worse, as it underestimates both bridge functions for  $r \lesssim 2R_g - 3R_g$ .

The RY optimization at  $\Phi_p = 0$  uses only the colloid-colloid correlations. Indeed, in this limit the consistency condition is

$$\left( \frac{\partial \beta P^{(\text{vir})}}{\partial \rho_c} \right)_{\rho_p=0} = 1 - \rho_c \hat{c}_{cc}(0). \quad (17)$$

Therefore, one might think that the relatively poor agreement for the polymer-polymer correlations for small values of  $r$  is related to the fact that the procedure does not take into account polymer properties. We have thus considered a two-parameter optimization. We set  $\chi_{pp} = \chi_1/R_g$  and  $\chi_{cc} = \chi_2/R_c$  as free parameters, while  $\chi_{pc}$  is, somewhat arbitrarily, set equal to  $(\chi_1 + \chi_2)/(R_g + R_c)$ . As consistency conditions, we consider Eq. (17) and [44]

$$\left( \frac{\partial \beta P^{(\text{vir})}}{\partial \rho_p} \right)_{\rho_c, \rho_p=0} = 1 - \rho_c \hat{c}_{cp}(0), \quad (18)$$

which involves polymer-colloid correlations. In Figs. 9 and 10, we also report the bridge functions for this case (they are labelled RY-2). For  $q = 1$  we observe a significant improvement with respect to the one-parameter RY case, although significant differences with Monte Carlo data are still present for  $r/R_g \lesssim 1$ . For  $q = 0.5$  instead, the two different RY closures yield equivalent estimates.

As a final case, we consider the RHNC closure, which relies on the assumption that the bridge functions can be accurately parametrized by those of a binary additive hard-sphere mixture. To verify if this is the

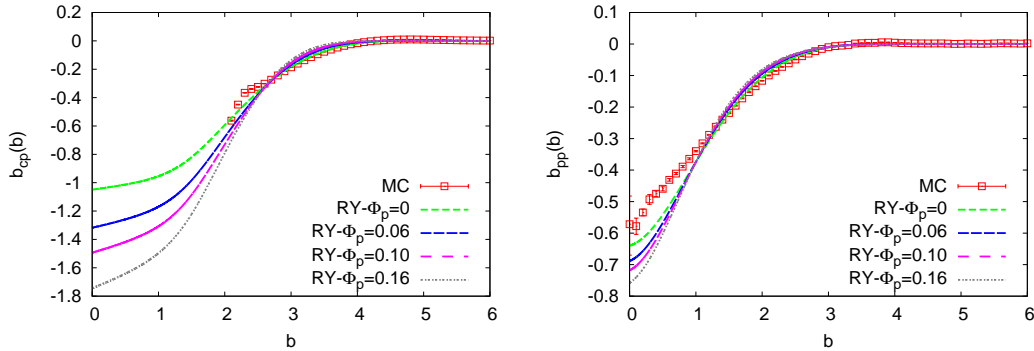


FIG. 11: Bridge functions for  $\Phi_c = 0.3$  and  $q = 0.5$  as a function of  $b = r/R_g$ . We report the zero-density function obtained by Monte Carlo simulations (MC), and the RY functions for different values of the polymer volume fraction  $\Phi_p$ .

case, we consider  $q = 0.5$  and  $\Phi_c = 0.3$ , and compute

$$\Delta(R_p) = \int |b_{pp}^{MC}(r) - b_{pp}^{HS}(r, R_p)| r^2 dr, \quad (19)$$

for different values of the effective polymer radius  $R_p$ . The optimal value (minimal  $\Delta$ ) is obtained for  $R_p = 0.842R_g$ . We can compare this result with that obtained by using the Lado criterion [20, 36]. For  $\Phi_p = 0$ , Eq. (6) is satisfied as we use the very accurate hard-sphere correlation function of Ref. [41]. To determine  $R_p$  one needs to consider the linear term in the polymer density, i.e., the equation

$$\int r^2 [h_{cp}(r) - h_{cp}^{HS}(r; R_p, R_c)] \frac{\partial b_{cp}^{HS}(r; R_p, R_c)}{\partial R_p} = 0. \quad (20)$$

Alternatively, one can determine  $R_p$  for several small values of  $\Phi_p$ , performing at the end an extrapolation to  $\Phi_p \rightarrow 0$ . The first method gives  $R_p = 0.837R_g$ , while the second one gives  $R_p = 0.828R_g$ . Both results are very close to the estimate  $R_p = 0.842R_g$  obtained by a direct matching of the bridge functions. This confirms that the Lado criterion provides the bridge functions that are the best approximations of the exact ones. The resulting bridge functions are reported in Fig. 10. The RHNC estimate of  $b_{cp}(r)$  is in agreement with the Monte Carlo function for  $r \gtrsim 2R_g$ . As for  $b_{pp}(r)$ , the RHNC estimate agrees with the Monte Carlo one for  $r \gtrsim R_g$ . At smaller distances, instead, the RHNC bridge function underestimates the correct one and appears to provide a worse approximation than the RY closure.

This analysis for  $\Phi_p = 0$  further confirms the results obtained in Sec. III B. For  $\Phi_c = 0.1$ , the bridge functions are quantitatively small, confirming the accuracy of the HNC approximation. On the other hand, for  $\Phi_c = 0.3$ , the RY closure is the one that provides the best approximation, while the HNC closure is the less accurate one as it cannot reproduce the small-distance behavior of the bridge functions. Note that, while  $b_{cp}(r)$  is correctly reproduced in the relevant region  $r \gtrsim R_c$ , the polymer-polymer bridge function is always poorly reproduced for  $r \lesssim R_g$ . This discrepancy gives rise to similar discrepancies in the correlation functions, as discussed in Sec. III B.

#### D. Integral equations with Monte Carlo bridge functions

As a final test we decided to determine the solutions of the integral equations by using the zero-density Monte Carlo bridge functions computed in Sec. III C. In other words, we consider the closure relation (2), setting for all values of  $\Phi_p$ ,  $b_{pp}(r; \Phi_c, \Phi_p) = b_{pp}^{MC}(r; \Phi_c, \Phi_p = 0)$ ,  $b_{cp}(r; \Phi_c, \Phi_p) = b_{cp}^{MC}(r; \Phi_c, \Phi_p = 0)$ , and  $b_{cc}(r; \Phi_c, \Phi_p) = b_{cc}^{HS}(r; \Phi_c)$ , where the last quantity is the bridge function of a pure hard-sphere system [43]. This approximation is exact for  $\Phi_p = 0$  and one may wonder whether it provides a reasonable approximation also for  $\Phi_p > 0$ . We have tested the approach for  $q = 0.5$  and  $\Phi_c = 0.3$ . The results for the structure factors, reported in Fig. 6 (they are labelled MC-B), show that this approach is only marginally better than that based on the HNC closure. Also the termination point,  $\Phi_p = 0.11$ , is only slightly above the HNC one,  $\Phi_p = 0.090$ .

To clarify the origin of the discrepancies, we have determined the RY bridge functions for several values of  $\Phi_p$ . As the RY estimates reasonably agree with the Monte Carlo data up to the termination line, we take them as estimates of the exact density-dependent  $b_{\alpha\beta}(r; \Phi_c, \Phi_p)$ . As one can see from the results shown in Fig. 11, the density dependence of the bridge functions is not large (for  $b_{cp}(r)$  the relevant region is  $b = r/R_g \gtrsim 2$ ). Yet, this relatively small difference is the cause of the different results obtained. In practice, this simple exercise shows that results are extremely sensitive to the specific form of the bridge functions in the colloid-liquid phase  $\Phi_c \gtrsim 0.25$ . Hence, accurate results can only be obtained by using accurate bridge functions, that none of the methods we investigated is able to provide.

#### IV. CONCLUSIONS

In the last years there has been a widespread interest in soft-matter systems characterized by the presence of macromolecules of mesoscopic size. In many situations, if one is only interested in the thermodynamic behavior or in structural properties on scales much larger than atomic distances, one can use coarse-grained (CG) models in which each macromolecule is represented by a single effective particle [10, 11, 17]. At variance with simple fluids for which potentials always have a hard core, in CG models potentials may be soft, allowing different effective molecules to overlap with a little energy penalty. Monocomponent CG models have been extensively studied [10, 11] by a variety of techniques. Among them, integral-equation methods have been proved to be very accurate. In particular, because of the soft nature of the interactions, the HNC and RY closures work quite well [29, 45]. It is then natural to investigate whether integral equations can be successfully applied to the study of the phase diagram and thermodynamics of more complex systems, for instance to mixtures of macromolecules and colloids, characterized by the simultaneous presence of soft and hard-core potentials.

In this paper, we consider a particular CG model, appropriate to describe long linear polymers interacting with hard-sphere colloids under good-solvent conditions, a well-studied paradigmatic model whose phase behavior has been extensively studied, see, e.g., Refs. [27, 46]. However, the conclusions should have general validity, applying to generic systems with soft and hard-core potentials. The phase diagram of the CG model has been discussed recently in Ref. [17]. The binodal curves and the critical points were determined for  $q = 0.5$  and  $q = 0.8$ , while, somewhat surprisingly, no sign of phase separation was found for  $q = 1$  up to relatively large polymer densities. Here, we have compared the Monte Carlo results with predictions obtained by using integral-equation methods and a variety of different closures: HNC, HNC/PY, RY, and RHNC.

For small values of  $\Phi_c$  we find that HNC is quite successful in predicting the correct thermodynamics and structure. On the other hand, for  $\Phi_c = 0.3$  (note that the critical point of the fluid-fluid transition is located at  $\Phi_{c,\text{crit}} = 0.25$  for both  $q = 0.5$  and  $0.8$ ) integral equations fail to converge well below the binodal line determined by Monte Carlo simulations. Below the termination line the RY closure is the one that fares best, reasonably reproducing the zero-momentum structure factors and the pair correlation functions. Nonetheless, RY integral equations stop converging at  $\Phi_p = 0.18, 0.39$  for  $\Phi_c = 0.3$  and  $q = 0.5, 0.8$ , respectively, while the binodal is located at significantly larger polymer densities, at  $\Phi_p = 0.38, 0.75$  for the same values of  $q$ .

The failure of integral equations to provide accurate estimates of the phase diagram is probably related to the strong nonadditivity of the model. Indeed, similarly large differences are observed in Ref. [16] for systems of nonadditive hard-sphere mixtures. If the system is asymmetric, i.e., for  $y \lesssim 0.6$  ( $y$  is the ratio of the diameters of the two spheres, a quantity which is the analog of  $q$ ), integral equations (and also density functional theory) are unable to provide quantitatively reliable results for the phase diagram. Moreover, discrepancies increase with the amount of asymmetry considered.

G.D. acknowledges support from the Italian Ministry of Education Grant PRIN 2010HXAW77. Computations were performed at the Pisa INFN Computer Center and at CINECA (ISCRA PHCOPY HP10CFFG8Q project).

#### Appendix A: Technical details

In the integral-equation approach, pair and direct correlation functions are discretized on  $N$  regularly spaced points,  $r_n = n\Delta r$ . Moreover, all functions are assumed to be zero at a cut-off distance  $R_{\text{max}} = N\Delta r$ . Typically, we take  $\Delta r = 0.001R_g$  and  $N = 32768$  or  $65536$ . The grid is extremely fine and reasonably large, to guarantee that results are stable with respect to the parameters  $\Delta r$  and  $N$ .

TABLE II: Estimates of the structure factors  $S_{\alpha\beta}(k=0)$ , of the concentration factor  $S_c(k)$ , of the virial pressure  $P^{(\text{vir})}$ , and of the compressibility  $\kappa_T$  computed using Eq. (12) for  $\Phi_c = 0.3$ ,  $\Phi_p = 0.09$ ,  $q = 0.5$ , and for the HNC closure. We report results for several values of  $N$  and  $\Delta r$ .

$\Delta r =$	$N = 32768$			$N = 65536$			
	0.001	0.002	0.004	0.0005	0.001	0.002	0.004
$\beta P^{(\text{vir})} R_c^3$	0.956	0.955	0.953	0.956	0.956	0.955	0.953
$\beta R_c^3 / \kappa_T$	1.763	1.762	1.756	1.764	1.763	1.761	1.756
$S_{pp}(0)$	3.399	3.436	3.560	3.384	3.399	3.436	3.560
$S_{cp}(0)$	-0.792	-0.801	-0.830	-0.788	-0.792	-0.801	-0.830
$S_{cc}(0)$	0.263	0.264	0.271	0.261	0.262	0.264	0.271
$S_c(0)$	0.396	0.400	0.414	0.393	0.396	0.400	0.414

In Table II we report several thermodynamic quantities as a function of  $\Delta r$  and  $N$  for the HNC closure at  $\Phi_c = 0.3$ ,  $\Phi_p = 0.09$ , a state point very close to the termination line.

Estimates do not change as  $N$  changes indicating that the cut-off distance is large enough. The step size is more crucial, but  $\Delta r = 0.001$  should be accurate enough. In the paper, most of the analysis use  $\Delta r = 0.001$  and  $N = 32768$ . In a few cases, we have checked the results, by changing  $\Delta r$  and/or  $N$  by a factor of 2. The independence of the results on the chosen parameters allows us to exclude that the observed behavior is due either to a too small cut-off distance or to a too coarse discretization of the correlation functions.

## Appendix B: Pair potentials

In this section we report the explicit expressions of the pair potentials. The model consists of coarse-grained polymers, represented as soft particles, and colloids. Polymers interact via a pair potential  $V_{pp}(b)$  given by [32]

$$\beta V_{pp}(b) = \sum_{i=1}^3 a_i \exp(-b^2/c_i^2), \quad (\text{B1})$$

where  $b = r/R_g$ ,  $a_1 = 0.999225$ ,  $a_2 = 1.1574$ ,  $a_3 = -0.38505$ ,  $c_1 = 1.24051$ ,  $c_2 = 0.85647$ , and  $c_3 = 0.551876$ . Colloids interact as hard spheres:

$$\begin{aligned} V_{cc}(r) &= 0 & r > 2R_c \\ V_{cc}(r) &= +\infty & r < 2R_c. \end{aligned} \quad (\text{B2})$$

The polymer-colloid pair potential depends on  $q$ . For small values of  $b = r/R_g$ , i.e. for  $b < b_{\min}$  ( $b_{\min} \approx R_c/R_g = 1/q$ ), the potential  $\beta V_{cp}(r; q)$  is large, hence it is impossible (and practically irrelevant) to estimate it accurately. For  $b \gtrsim b_{\min}$  we parametrize it as

$$\beta V_{cp}(r; q) = a_1(q) e^{-[(b-c_1(q))/e_1(q)]^2} + a_2(q) e^{-[|b-c_2(q)|/e_2(q)]^{d_2(q)}}, \quad (\text{B3})$$

TABLE III: Coefficients parametrizing  $\beta V_{cp}(r; q)$  for different values of  $q$ . The parametrization is accurate for  $1.91 \leq b \leq 5.38$ ,  $0.90 \leq b \leq 4.54$ , and  $0.47 \leq b \leq 4.28$  for  $q = 0.5, 0.8, 1$ , respectively.

$q$	$a_1$	$e_1$	$c_1$	$a_2$	$e_2$	$c_2$	$d_2$
0.5	0.634486	0.305183	2.13936	15.1368	0.512611	1.629090	1.30679
0.8	0.411558	0.318504	1.40563	13.5385	0.728577	0.572266	1.56655
1.0	0.982437	0.496784	0.98100	14.1753	0.84914	0	1.6023262

where  $b = r/R_g$ . Estimates of the coefficients are reported in Table III. To verify the accuracy of the parametrization, we compare the estimate of  $A_{2,cp} = B_{2,cp}/R_g^3$  ( $B_{2,cp}$  is the second polymer-colloid virial coefficient) obtained by using the parametrized potential and the estimate of the same quantity in the full-monomer model [34]. Using the parametrized potentials we obtain  $A_{2,cp} = 106.79, 41.52, 27.50$  for  $q = 0.5, 0.8, \text{ and } 1$ , respectively, to be compared with the full-monomer results  $A_{2,cp} = 107.4(3), 41.7(1), 27.54(6)$ . Differences are small (they are less than 0.6%), confirming the accuracy of the results.

- 
- [1] J. P. Hansen and I. McDonald, *Theory of Simple Liquids with Applications to Soft Matter*, 4th ed. (Academic Press, Amsterdam, 2013).
- [2] P. Attard, *Thermodynamics and Statistical Mechanics: Equilibrium by Entropy Maximization*, (Academic Press, London, 2002).
- [3] M. Mézard and G. Parisi, J. Phys. A **29**, 6515 (1996).  
M. Mézard and G. Parisi, J. Chem. Phys. **111**, 1076 (1999).
- [4] G. Parisi and F. Zamponi, Rev. Mod. Phys. **82**, 789 (2010).
- [5] J.-M. Bomont, J.-P. Hansen, and G. Pastore, J. Chem. Phys. **141**, 174505 (2014).
- [6] P. T. Cummings and G. Stell, J. Chem. Phys. **78**, 1917 (1983).
- [7] L. Belloni, J. Chem. Phys. **98**, 8080 (1993).
- [8] R. F. Rull, C. Vega, and S. Lago, Mol. Phys. **87**, 1235 (1996).
- [9] G. Sarkisov and E. Lomba, J. Chem. Phys. **122**, 214504 (2005).
- [10] C. N. Likos, Phys. Rep. **348**, 267 (2001).
- [11] J.-P. Hansen and H. Löwen, in *Bridging Time Scales: Molecular Simulations for the Next Decade*, Lect. Notes Phys. **605**, edited by P. Nielaba, M. Mareschal, and G. Ciccotti (Springer, Berlin-Heidelberg, 2002) p. 167.
- [12] A. A. Louis, R. Finken, and J. P. Hansen, Phys. Rev. E **61**, R1028 (2000).
- [13] J. Dzubiella, C. N. Likos, and H. Löwen, J. Chem. Phys. **116**, 9518 (2002).
- [14] R. Finken, J. P. Hansen, and A. A. Louis, J. Stat. Phys. **110**, 1015 (2003).
- [15] G. Pellicane, F. Saija, C. Caccamo, and P. V. Giaquinta, J. Phys. Chem. B **110**, 4359 (2006).
- [16] G. Pellicane and O. G. Pandaram, J. Chem. Phys. **141**, 044508 (2014).
- [17] G. D'Adamo, R. Menichetti, A. Pelissetto, and C. Pierleoni, arXiv:1501.01046.
- [18] F. J. Rogers and D. A. Young, Phys. Rev. A **30**, 999 (1984).
- [19] Y. Rosenfeld and N. W. Ashcroft, Phys. Rev. A **20**, 1208 (1979).
- [20] E. Enciso, F. Lado, M. Lombardero, J. L. F. Abascal, and S. Lago, J. Chem. Phys. **87**, 2249 (1984).
- [21] W. C. K. Poon, J. Phys.: Condensed Matter **14**, R859 (2002).
- [22] M. Fuchs and K. S. Schweizer, J. Phys.: Condensed Matter **14**, R239 (2002).
- [23] R. Tuinier, J. Rieger, and C. G. de Kruif, Adv. Coll. Interface Sci. **103**, 1 (2003).
- [24] K. J. Mutch, J. S. van Duijneveldt, and J. Eastoe, Soft Matter **3**, 155 (2007).
- [25] G. J. Fleer and R. Tuinier, Adv. Coll. Interface Sci. **143**, 1 (2008).
- [26] O. Myakonkaya and J. Eastoe, Adv. Coll. Interface Sci. **149**, 39 (2009).
- [27] H. N. W. Lekkerkerker and R. Tuinier, *Colloids and the Depletion Interaction*, Lect. Notes Phys. **833** (Springer, Berlin, 2011).
- [28] G. D'Adamo, A. Pelissetto, and C. Pierleoni, J. Chem. Phys. **141** (2014) 244905.
- [29] A. A. Louis, P. G. Bolhuis, J. P. Hansen, and E. J. Meijer, Phys. Rev. Lett. **85**, 2522 (2000); P. G. Bolhuis, A. A. Louis, J. P. Hansen, and E. J. Meijer, J. Chem. Phys. **114**, 4296 (2001).
- [30] A. A. Louis, P. G. Bolhuis, E. J. Meijer, and J. P. Hansen, J. Chem. Phys. **116**, 10547 (2002).
- [31] A. A. Louis, P. G. Bolhuis, E. J. Meijer, and J. P. Hansen, J. Chem. Phys. **117**, 1893 (2002).
- [32] A. Pelissetto and J. P. Hansen, J. Chem. Phys. **122**, 134904 (2005).
- [33] A. Pelissetto and J. P. Hansen, Macromolecules **39**, 9571 (2006).
- [34] G. D'Adamo, A. Pelissetto, and C. Pierleoni, Mol. Phys. **111**, 3372 (2013).
- [35] T. Biben and J. P. Hansen, J. Phys.: Condens. Matter **3**, F65 (1991).
- [36] F. Lado, Phys. Lett. A **89**, 196 (1982).
- [37] J. L. Lebowitz, Phys. Rev. A **133**, 895 (1964).
- [38] J. L. Lebowitz, G. Helfand, and E. Praestgaard, J. Chem. Phys. **43**, 774 (1965).
- [39] G. A. Mansoori, N. F. Carnahan, K. E. Starling, and T. W. Leland, Jr., J. Chem. Phys. **54**, 1523 (1971).
- [40] L. Verlet and J. J. Weis, Phys. Rev. A **5**, 939 (1972).
- [41] E. W. Grundke and D. Henderson, Mol. Phys. **24**, 269 (1972).
- [42] L. L. Lee and D. Levesque, Mol. Phys. **26**, 1351 (1973).
- [43] D. Henderson and E. W. Grundke, J. Chem. Phys. **63**, 601 (1975).
- [44] A. Ben-Naim, *Molecular Theory of Solutions* (Oxford Univ. Press, Oxford, 2006).
- [45] M. Watzlawek, H. Löwen, and C. N. Likos, J. Phys.: Condens. Matter **10**, 8189 (1998).
- [46] G. D'Adamo, A. Pelissetto, and C. Pierleoni, J. Chem. Phys. **141**, 024902 (2014).